# Histochemical characterization of TDAG51 in endothelial remodeling and angiogenesis following myocardial infarction *via* PI3K-AKT signaling

Kaizheng Liu,[1]* Jinyu Pan,[1]* Quan Liu,[1] Yang Huang,[1] Liqun Shang,[1] Yi Zhang,[1] Jinming Wen,[2] Huayang Li,[1] Zhongkai Wu[1]

[1]Department of Cardiac Surgery, First Affiliated Hospital of Sun Yat-sen University, Guangzhou
[2]School of Statistics, Renmin University of China, Beijing, China

*These authors contributed equally to this work

ABSTRACT

Myocardial infarction (MI) triggers complex cardiac remodeling, including endothelial dysfunction, fibrosis, and angiogenesis. Characterizing the spatial distribution and cellular localization of regulatory molecules is critical for understanding cardiac repair mechanisms. This study investigated the histochemical localization and functional role of T-cell death-associated gene 51 (TDAG51) in endothelial cells during post-MI angiogenesis and cardiac remodeling. We established a murine MI model and silenced TDAG51 with adeno-associated virus. Histochemical assays were used to determine TDAG51 localization and its relation to vascular density, and Masson staining was used to evaluate myocardial fibrosis. *In vitro*, we exposed human coronary artery endothelial cells (HCAECs) to oxygen-glucose deprivation (OGD) to examine TDAG51 expression and endothelial function. We performed Western blot and transcriptomic analyses to explore the involvement of the PI3K-AKT signaling pathway. Histochemical analyses revealed that TDAG51 was predominantly localized in CD31-positive endothelial cells and was significantly upregulated in the infarcted myocardium, particularly in the peri-infarct regions. TDAG51 silencing markedly increased capillary density and reduced fibrotic area, as demonstrated by immunohistochemistry and Masson staining. *In vitro*, TDAG51 knockdown enhanced endothelial proliferation, migration, and tube formation. Mechanistically, these effects were associated with activation of the PI3K-AKT signaling pathway, while pharmacological inhibition of PI3K attenuated the pro-angiogenic phenotype. This study provides histochemical evidence that TDAG51 is enriched in ischemic myocardial endothelial cells and negatively regulates angiogenesis. TDAG51 inhibition promotes vascular remodeling and enhances cardiac repair following myocardial infarction, highlighting TDAG51 as a promising therapeutic target for improving post-MI recovery.

**Correspondence:** Zhongkai Wu, Department of Cardiac Surgery, First Affiliated Hospital of Sun Yat-Sen University, 58 Zhongshan II Rd, Guangzhou 510080, China. E- mail: wuzhk@mail.sysu.edu.cn
Huayang Li, Department of Cardiac Surgery, First Affiliated Hospital of Sun Yat-Sen University, 58 Zhongshan II Rd, Guangzhou 510080, China. E-mail: lihuayang94@163.com

**Contributions:** Kaizheng Liu, data curation, conceptualization, investigation, methodology, project administration, validation, visualization, writing – original draft, writing – review & editing. Jinyu Pan, formal analysis, investigation, methodology, validation, visualization. Quan Liu, formal analysis, methodology, supervision. Yang Huang, formal analysis, methodology. Liqun Shang, formal analysis, methodology. Yi Zhang, formal analysis, methodology. Jinming Wen, formal analysis, methodology. Huayang Li, conceptualization, investigation, methodology, project administration, supervision, writing – original draft, writing – review & editing. Zhongkai Wu, conceptualization, funding acquisition, project administration, resources, supervision, writing – original draft, writing – review & editing. All authors read and approved the final manuscript.

**Ethics approval:** all animal experiments were carried out with the approval of the Institutional Animal Care and Use Committee (IACUC) of Sun Yat-Sen University (Approval No. SYSU-IACUC-2020-000510).

**Funding:** this work was supported by the National Natural Science Foundation of China (Grant number: 82370271; 82070297).

**Conflict of interest:** the authors declare that the research was conducted without any potential conflict of interest stemming from commercial or financial relationships.

**Data Availability Statement**: the datasets generated for this study are available on reasonable request to the corresponding authors.

## Introduction

Mortality from cardiovascular diseases (CVDs) has been increasing recently, accounting for approximately one-third of all deaths in the population and has posed a hefty burden to the social economy, according to the American Heart Association.[1-3] Myocardial infarction (MI) is one of the most fatal CVDs with high rates of morbidity and mortality.[4] Since the pathological feature of MI is poor cardiac blood perfusion, restoring blood flow is the most effective means to limit the damage to ischemic tissues. In the treatment of ischemic heart disease, therapeutic angiogenesis has been extensively explored.[5] The latter plays a fundamental role in promoting myocardial infarction repair and preventing adverse ventricular remodeling. Therefore, identifying key regulators of angiogenesis as therapeutic targets to promote blood flow recovery after MI is of great interest.[6,7]

T-cell death-associated gene 51 (TDAG51), a member of the pleckstrin homology-like domain family, is known to be upregulated in response to endoplasmic reticulum stress and has been shown to induce apoptosis when overexpressed.[8,9] The TDAG51 gene is a cloned gene related to apoptosis from T cells, which is widely expressed in various tissues in the body, such as the brain, kidneys, and heart.[8,10] The expression of the TDAG51 gene is lower in tumor tissue compared to normal tissue, and constitutive expression of the TDAG51 gene can inhibit tumor growth.[11] Some studies suggest that the TDAG51 gene is involved in the formation of atherosclerosis. In endothelial cells, TDAG51 gene expression can be induced by homocysteine that induces apoptosis in vascular endothelial cells.[12] There is a close relationship between apoptosis and angiogenesis, and both biological processes play an important role in maintaining the normal physiological state of tissues and organs as well as in the development of diseases.[13] Therefore, we speculate that TDAG51 may also inhibit the growth and proliferation of vascular endothelial cells. Recent studies have demonstrated that TDAG51 is critically involved in multiple cardiovascular disorders, including vascular calcification, atherosclerosis, and renal interstitial fibrosis, mainly by regulating apoptosis, inflammation, and extracellular matrix deposition.[14,15] However, whether TDAG51 regulates angiogenesis and post-myocardial infarction (MI) cardiac repair remains elusive. In the present study, we aimed to explore the role and underlying mechanisms of TDAG51 in cardiac repair during MI.

In the present work, we investigated the effects of TDAG51 on human coronary artery endothelial cells (HCAECs) and ischemic heart. We showed that the migratory ability, angiogenic function, and proliferation of HCAECs were rescued by TDAG51 knockdown. Moreover, TDAG51 knock-down exhibited a strong cardioprotective effect on MI heart by promoting neo vessel formation in the ischemic border zone.

## Materials and Methods

### Animals

Male wild-type C57BL/6 mice (22-25 g, 6-8 weeks old) were procured from the Guangdong Province Animal Center in Guangzhou, PR China, and were housed within the experimental animal center at Sun Yat-Sen University, Guangzhou, PR China. All animal experiments were carried out with the approval of the Institutional Animal Care and Use Committee (IACUC) of Sun Yat-Sen University (Approval No. SYSU-IACUC-2024-001124). The mice were maintained in a specific pathogen-free (SPF)-grade facility, where they were subjected to a 12-h light and 12-h dark cycle, with ambient conditions of 24±1°C temperature and 50–60% relative humidity. They were provided with ad libitum access to both food and water throughout the study period. All perioperative care and surgical procedures adhered to the animal care protocols established by Sun Yat-Sen University (Protocol No. 2017-692) and were in compliance with the guidelines outlined in the «Guide for the Care and Use of Laboratory Animals» as published by the National Institutes of Health.

### Cell culture

Human coronary artery endothelial cells were procured from Cell Applications Inc. (Catalog 300-5, Lot 2989; Beijing, China) and were cultivated in endothelial cell medium (ECM) (#1001; ScienCell, San Diego, CA, USA) within humidified $CO_2$ incubators set at 37°C. The ECM formulation consisted of basal DMEM supplemented with 5% fetal bovine serum (FBS, #0025; ScienCell), 1% endothelial growth factor (ECGS, #1052; ScienCell), and 1% penicillin/streptomycin solution (P/S, #0503; ScienCell). Cells were expanded and cryopreserved in liquid nitrogen for subsequent experimental utilization. Medium replenishment was performed every 2 days, and upon reaching confluence, cells were detached using EDTA/trypsin and subsequently seeded into new Corning cell culture plates at ratios of 1:3 or 1:4.

### Construction and infection of adeno-associated virus

Adeno-associated virus (AAV) vectors were constructed by Puzhou Gene Technology (Guangzhou, China). To test the effects of TDAG51 in MI mice, serotype 9 AAV were used for TDAG51 knockdown in hearts. Six-week-old mice were chosen to receive a single bolus local injection of AAV9 at $1\times10^{11}$ viral genomes per mouse. Model was performed after 2 weeks of infection.

### siRNA intervention

To achieve the knockdown of TDAG51, HCAECs were transfected with TDAG51-siRNA (Zixi Biotech, Beijing, China) or control siRNA (Zixi Biotech) using the Lipofectamine RNAiMAX Reagent Kit (13778030; Invitrogen, Carlsbad, CA, USA) following the manufacturer's recommended protocol. Transfection efficiency was assessed through Western blotting conducted 48 h post-transfection.

### Western blot analysis

Cellular protein was extracted utilizing RIPA lysis buffer (Beyotime Biotechnology, Shanghai, China) supplemented with a cocktail of protease and phosphorylase inhibitors (Merck Millipore, Billerica, MA, USA). The protein concentration was determined using a Bio-Rad protein assay kit (Bio-Rad Laboratories, Hercules, CA, USA). SDS-PAGEs of 10-12% were employed to fractionate the entire lysate, which was subsequently transferred onto PVDF membranes (Merck Millipore). Following a 1-h blocking step with 5% BSA, the membranes were incubated overnight at 4°C with primary antibodies targeting TDAG51 (No. sc-23866, 1:100; Santa Cruz Biotechnology, Santa Cruz, CA, USA), AKT (No. 4685s, 1:1,000; Cell Signaling Technology, Danvers, MA, USA), phospho-AKT (No. 4060s, 1:1,000; Cell Signaling Technology), PI3K (No. AF6241, 1:1,000; Affinity Biosciences, Beijing, China), phospho-PI3K (No. AF3241, 1:1,000; Affinity Biosciences), and GAPDH (No. 60004-1-Ig, 1:3,000; Proteintech, Rosemont, IL, USA). On the subsequent day, the membranes were exposed to the appropriate peroxidase-conjugated secondary antibodies (SouthernBiotech, Birmingham, AL,

USA) for 1 h. Protein bands were visualized using the Western chemiluminescent HRP substrate (Merck Millipore) and ChemiDoc Touch system (Bio-Rad Laboratories).

## RNA extraction and qPCR

Total RNA was extracted from HCAECs utilizing TRIzol reagent (Catalog No. T9424; Sigma-Aldrich, St. Louis, MO, USA) following the manufacturer's protocols. Subsequently, reverse transcription was conducted using the PrimeScript RT reagent Kit (Catalog No. RR036A; TaKaRa, Tokyo, Japan). Quantitative real-time PCR was performed using SYBR-Green Master mix (Catalog No. RR820B; TaKaRa) on a LightCycle480 II instrument (Roche, Basel, Switzerland). For normalization, β-actin was employed as the internal reference gene. The primer sequences utilized in this study were as follows: β-actin: Forward 5'-ACAGAGCCTCGCCTTTGC-3' and Reverse 5'- GATATCATCATCCATGGTGAGCTGG -3' TDAG51: Forward 5'-CCGGGCAAGACAAGGTTTTGA-3' and Reverse 5'-GGGCGGAGAGACTGTTTTGC-3'

## OGD model establishment *in vitro*

The oxygen-glucose deprivation (OGD) model was established to replicate the microenvironment of HCAECs *in vitro*. HCAECs in the logarithmic growth phase were harvested and subjected to three washes with glucose-free DMEM (Thermo Fisher Scientific, Inc., Waltham, MA, USA). Subsequently, the original medium was replaced with glucose-free DMEM, and the cells were transferred to an incubator set at 1% $O_2$, 5% $CO_2$, and 94% $N_2$ for 24 hours at 37°C.

## LY294002 for PI3K inhibition

LY294002 (dissolved in DMSO vehicle; Sigma Aldrich) was employed to inhibit PI3K activity.[16] The control group received an equivalent volume of DMSO as a vehicle control. Forty-eight hours after cell seeding, Human HCAECs were treated for 2 h at 37°C in a 5% $CO_2$ environment with various cell supernatants containing 10 μM LY294002 to suppress PI3K activity. Subsequently, Western blot analysis was conducted.

## Cell proliferation assay

The EdU Cell Proliferation Kit with Alexa Fluor 555 (Catalog No. C0075; Beyotime) assay was employed to evaluate the proliferation of HCAECs, following the manufacturer's instructions. HCAECs were seeded at a density of 20,000 cells per well in 24-well plates, with each well containing 500 μL of ECM. The cells were then incubated for 24 h. After incubation, the cells were treated with a 10 μM EdU solution for 2 h, followed by fixation with 4% paraformaldehyde and subsequent staining with DAPI (Catalog No. C1002; Beyotime). Images were randomly selected and captured at ×100 magnification using a microscope (DMI8; Leica Wetzlar, Germany). Four random fields were chosen for each well.

## Wound healing assay

A wound healing assay was employed to evaluate the migratory capabilities of HCAECs. Approximately $4\times10^5$ cells were seeded in a six-well plate and cultivated in complete ECM medium until confluence was reached. Subsequently, a 200 μL pipette tip was used to directly create a wide noncellular area by scratching through the cell monolayer, followed by three washes with PBS to eliminate cell debris resulting from the scratch. To ensure consistent field of view, the cover of the six-well plate was marked. The medium was then replaced with cultured DMEM containing 1% fetal calf serum. Observations of the scratches for each experimental group were made under an inverted phase-contrast microscope at both 0 hours and 24 hours. The area of the scratch was quantified using ImageJ software (National Institutes of Health, Bethesda, MD, USA).

## Tube formation assay

Initially, 50 μL of growth factor-reduced Matrigel (BD Biosciences, Franklin Lakes, NJ, USA) was added to 96-well plates and subsequently incubated in an incubator for 30 min at 37°C. HCAECs were prepared at the appropriate concentration and seeded at a density of 50,000 cells per well in a 96-well plate. Following Matrigel solidification, the plate was maintained at 37°C. After an 8-h incubation period, images of tube formation were captured using an inverted microscope from Olympus (Tokyo, Japan). Subsequently, ImageJ Pro software was utilized to quantify the number of interconnecting tubes in each experimental group.

## *In vivo* model of myocardial infarction

According to previous methods,[18-21] male C57BL/6 mice, aged 8-9 weeks, were anesthetized via intraperitoneal injection of 50 mg/kg sodium pentobarbital. Subsequently, they were mechanically ventilated using a volume-regulated respirator (SAR830; Cwe Inc., Fullerton, CA, USA) To induce MI, the left anterior descending (LAD) coronary artery was permanently ligated with an 8-0 Prolene suture. In the sham group, an analogous procedure was conducted, albeit with a loosely placed suture at the same anatomical location.

## Echocardiography

Transthoracic echocardiography was performed on anesthetized male C57BL/6 mice utilizing a Visual Sonics system (Toronto, ON, Canada). M-mode and two-dimensional echocardiography were conducted to assess left ventricular ejection fraction (LVEF).

## Masson staining

The heart was carefully dissected, fixed in 4% paraformaldehyde for a duration of 24 hours, and subsequently embedded in paraffin before being sectioned. The heart sections underwent Masson trichromatic staining for histological assessment. Light microscopy (Carl Zeiss, Jena, Germany) was employed to conduct an overall histological evaluation.

## Immunohistochemical staining

For immunohistochemical (HIC) analysis, fresh frozen tissue sections were fixed with 4% paraformaldehyde, followed by permeabilization in 0.4% Triton X-100 (Sigma-Aldrich). Subsequently, the sections were stained with primary antibodies against CD31 (dilution 1:200, ab182981). To detect the primary antibodies, fluorescent conjugated secondary antibodies were utilized. Nuclei were counterstained with DAPI. Quantification was performed by analyzing three microscopic fields within the border areas of the left ventricle (LV) for each section using Image J software. The peri-infarct region was defined as a 0.5~1 mm wide zone adjacent to the fibrous scar in the left ventricular free wall. Three non-overlapping fields in this region were randomly captured for quantification.

## Immunofluorescence staining

Immunofluorescence staining was conducted following the specified protocol. Upon permeabilization with 0.1% Triton X-100 in PBS, cover slides containing differently treated heart sections were subjected to a 30-minute blocking step with 10% bovine serum albumin. After two subsequent washes with PBS, the samples were

incubated overnight at 4°C with the following primary antibodies: anti-CD31 (ab182981; Abcam, Cambridge, MA, USA) and anti-TDAG51 (sc-23866; Santa Cruz Biotechnology). Following another round of PBS washes, the samples were incubated with the corresponding fluorescent secondary antibodies. Finally, the slides were mounted with DAPI and subjected to imaging.

### Statistical analysis

Data are presented as means ±SD. Statistical analyses were conducted using GraphPad Prism 8 software (GraphPad Software, Inc., La Jolla, CA, USA). The data were normalized to the control group, and no data points were excluded from any of the experiments. Group comparisons were performed utilizing one-way ANOVA followed by Bonferroni's test for multiple comparisons. For comparisons between two groups, an unpaired two-tailed Student's *t*-test was used. A *p*-value of less than 0.05 was considered statistically significant.

## Results

### Increased TDAG51 expression in myocardial infarction

Two weeks after MI modeling, mouse hearts were harvested, embedded, and sectioned for immunofluorescence staining of CD31 and TDAG51. As shown in Figure 1A, TDAG51 colocalized with CD31, indicating its predominant expression in endothelial cells. Moreover, TDAG51 expression was markedly increased in the infarcted hearts. *In vitro*, the purity of isolated primary endothelial cells was verified by CD31 immunofluorescence staining (Figure 1B). HCAECs were then subjected to OGD, followed by Western blot analysis to assess TDAG51 expression. As shown in Figure 1C, TDAG51 expression was significantly upregulated in HCAECs following OGD treatment. These findings suggest a potential role for TDAG51 in the vascular response to myocardial infarction.

### Impact of TDAG51 knock-down on endothelial cell function and vascular homeostasis

We silenced TDAG51 expression in HCAECs *via* siRNA transfection. As shown in Figure 2A, both siRNA-2 and siRNA-3 significantly reduced TDAG51 mRNA levels. siRNA-3 was selected for subsequent experiments due to its superior knockdown efficiency. Western blot analysis confirmed that siRNA-3 effectively decreased TDAG51 protein expression in HCAECs (Figure 2B).

To comprehensively investigate the role of TDAG51 in HCAECs, RNA sequencing was performed following TDAG51 knockdown. A total of 1,891 differentially expressed genes (DEGs) were identified, including 810 upregulated and 1,081 downregulated genes (|log2 fold change| >1 and adjusted $p<0.05$; Figure 2C). Transcriptomic profiling revealed that TDAG51 knockdown altered the expression of genes involved in endothelial barrier integrity and vascular homeostasis (Figure 2D). Notably, genes regulating vascu-

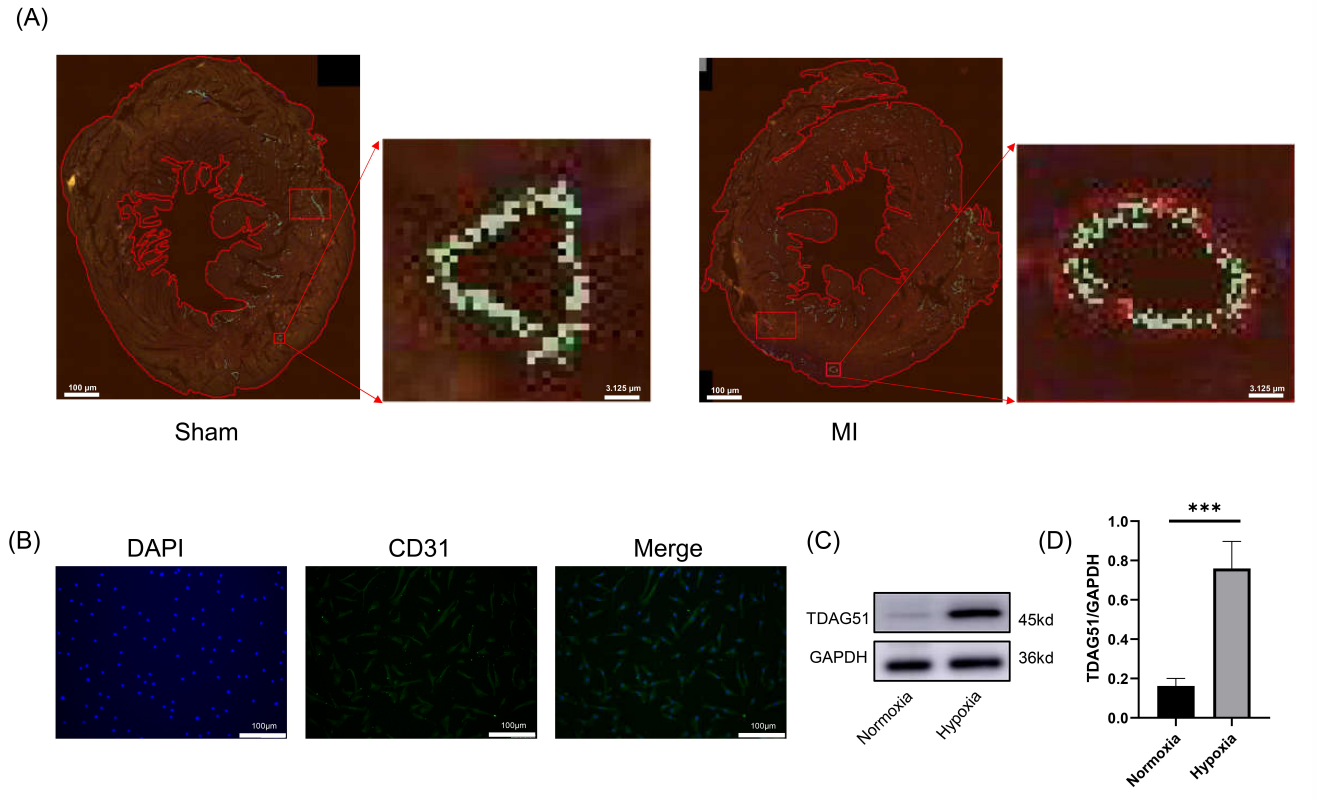


**Figure 1.** Hypoxia induces upregulation of TDAG51 expression in endothelial cells. **A**) Representative confocal microscopy images of TDAG51 (red) and CD31 (green) co-expressed in cardiac infarct zone. **B**) Identification of coronary endothelium derived from coronary arteries of heart transplant patients. **C**) Representative images of Western blot. **D**) The ratio of TDAG51 to GAPDH under normoxia and hypoxic conditions (n=3). TDAG51 showed consistent co-localization with CD31-positive endothelial cells in all analyzed fields (n=3 biological replicates), supporting its predominant endothelial distribution. ***$p<0.001$.

lar permeability and endothelial junctions were significantly altered, indicating that TDAG51 modulates endothelial barrier function. Genes related to metabolism and oxidative stress were also affected, suggesting a role in metabolic and redox balance. KEGG (Kyoto Encyclopedia of Genes and Genomes) pathway analysis further demonstrated significant enrichment of DEGs in the PI3K-AKT signaling pathway (Figure 2E).

## TDAG51 knock-down promoted angiogenesis *in vitro*

The PI3K/Akt/mTOR signaling pathway is a well-established regulator of angiogenesis following MI.[22] Our RNA-seq data showed significant enrichment in this pathway; we therefore examined PI3K-AKT activation after TDAG51 knockdown in HCAECs. As shown in Figure 3A, TDAG51 silencing markedly increased the expression of phosphorylated AKT (p-AKT) and phosphorylated PI3K (p-PI3K), while total AKT and PI3K levels remained unchanged, indicating activation of the PI3K-AKT signaling cascade. Functionally, TDAG51 suppression significantly enhanced endothelial cell proliferation, as evidenced by a greater number of EdU-positive cells compared to the control group (Figure 3B). Wound healing assays demonstrated that TDAG51 knockdown significantly promoted HCAEC migration (Figure 3C). Furthermore, tube formation assays revealed that silencing TDAG51 significantly enhanced the cells' ability to form capil-

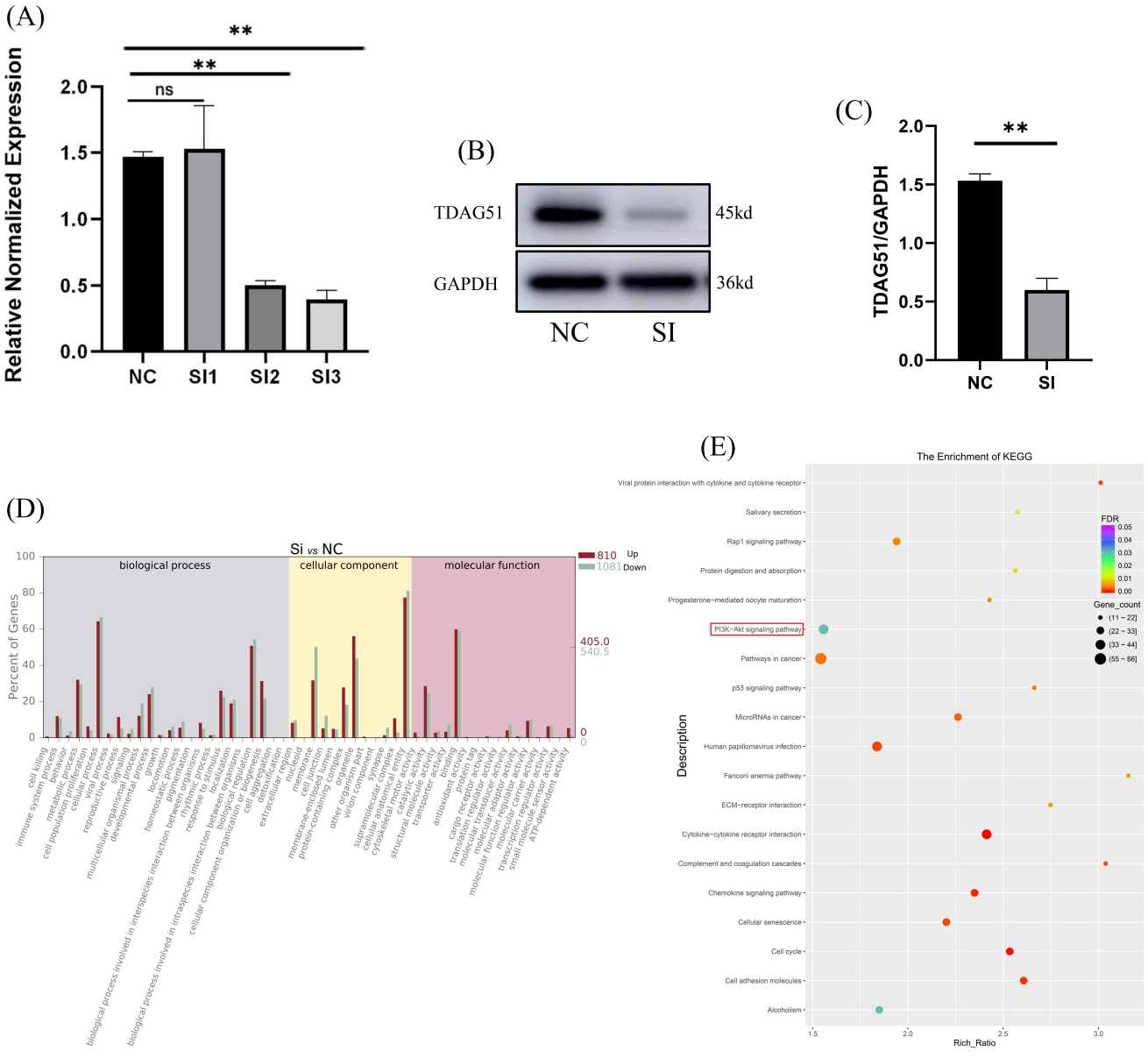


**Figure 2.** RNA sequencing profiling of endothelial cells with TDAG51 knock-down. **A**) qPCR analysis of TDAG51 mRNA level (n=3). **B**) Representative images of Western blot. **C**) Determine the TDAG51/GAPDH ratio based on Western blot (n=3). **D**) GO (Gene Ontology) analysis of the DEGs. **E**) KEGG (Kyoto Encyclopedia of Genes and Genomes) pathway analysis of the DEGs. Transcriptomic analysis reveals that TDAG51 knockdown extensively affects vascular homeostasis-related genes and significantly enriches the PI3K-AKT signaling pathway. $^{ns}p>0.05$, $^{**}p<0.01$.

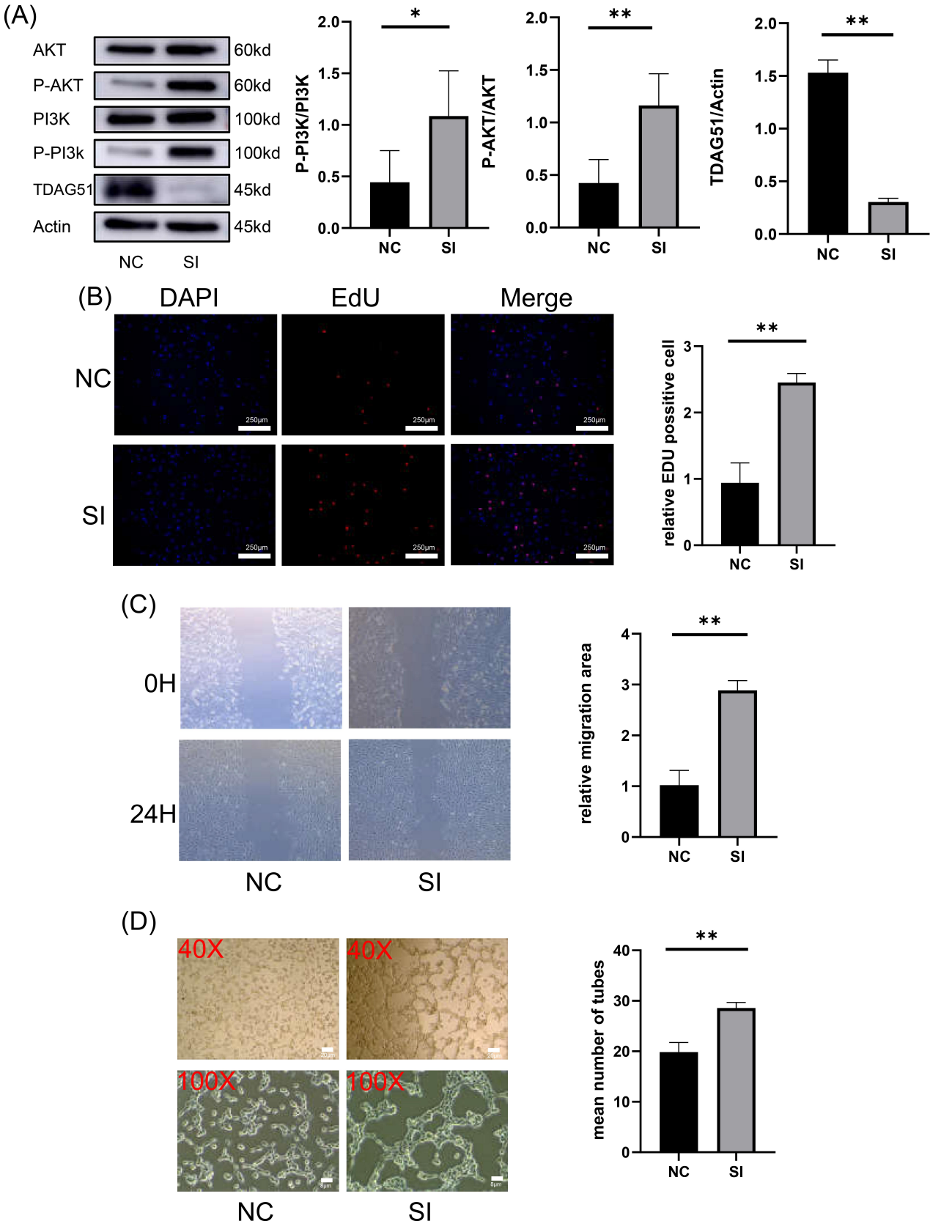


**Figure 3.** TDAG51 knock-down enhances angiogenesis *in vivo*. **A**) Representative images and quantitative analysis of Western blot (n=3). **B**) Representative images and quantitative analysis of EdU cell proliferation assay (n=5). **C**) Representative images and quantitative analysis of cell scratch assay (n=5). **D**) Representative images and quantitative analysis of tube formation assay (n=5). These functional assays confirm that TDAG51 negatively regulates endothelial angiogenic capacity *in vitro*. *$p$<0.05, ** $p$<0.01.

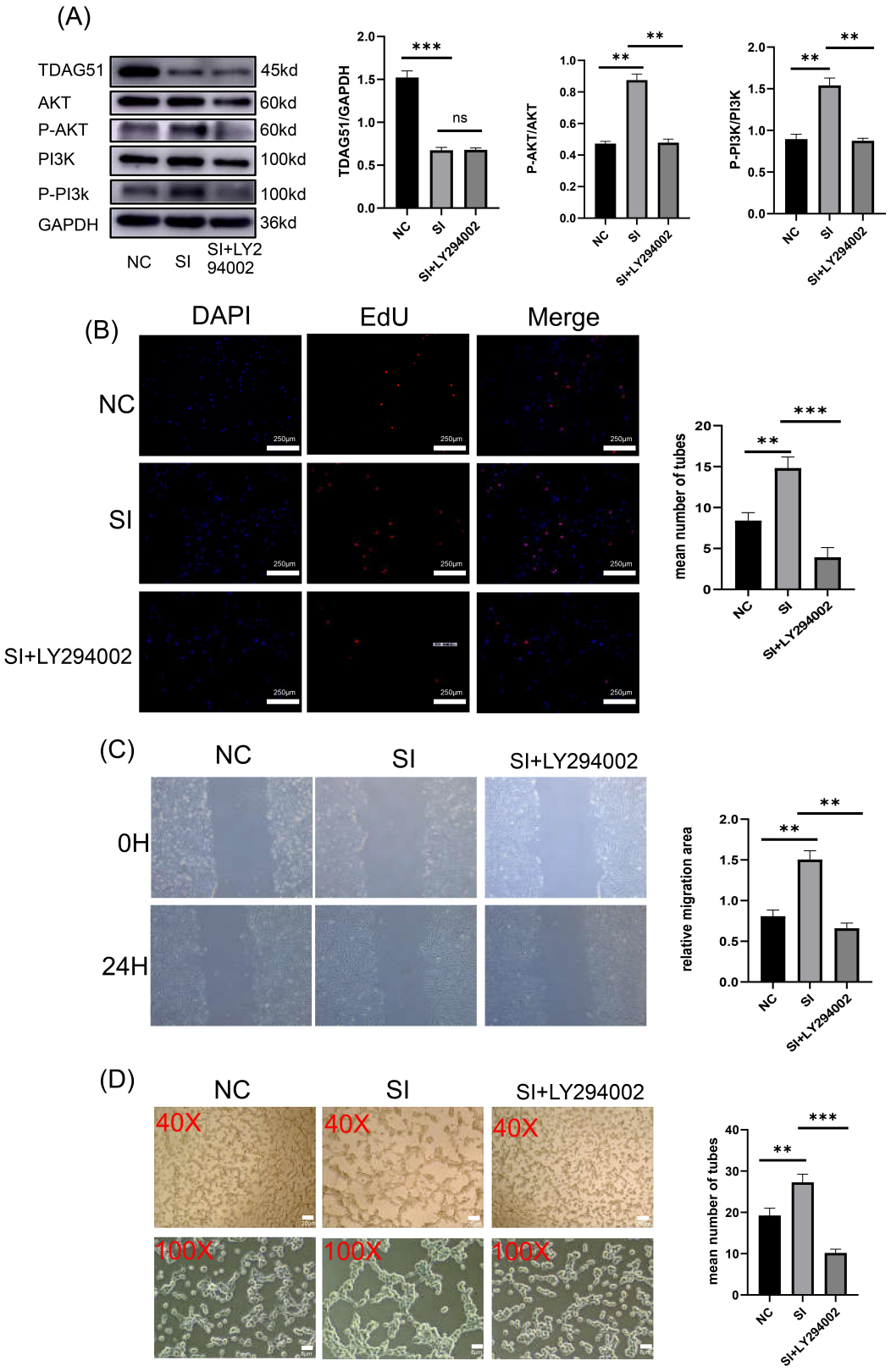


**Figure 4.** TDAG51 knock-down enhances angiogenesis *in vivo via* PI3K/AKT pathway activation. **A**) Representative images and quantitative analysis of Western blot (n=3). B) Representative images and quantitative analysis of EdU cell proliferation assay (n=5). **C**) Representative images and quantitative analysis of cell scratch assay (n=5). **D**) Representative images and quantitative analysis of tube formation assay (n=5). These data confirm that the PI3K-AKT pathway is essential for TDAG51-mediated regulation of endothelial function. $^{ns}p>0.05$, $^{**}p<0.01$, $^{***}p<0.001$.

lary-like structures in vitro (Figure 3D). Collectively, these results indicate that TDAG51 negatively regulates endothelial proliferation, migration, and angiogenesis. Its knockdown promotes angiogenesis *in vitro* and may represent a therapeutic strategy for ischemic heart disease.

## TDAG51 knock-down regulates angiogenesis of human coronary endothelial cells *via* the PI3K-AKT pathway

To determine whether the pro-angiogenic effects of TDAG51 knockdown in HCAECs are mediated through activation of the PI3K-AKT signaling pathway, we employed LY294002, a specific PI3K inhibitor, to suppress pathway activation. As anticipated, treatment with LY294002 effectively inhibited the TDAG51 knockdown-induced phosphorylation of PI3K and AKT (Figure 4A). Subsequently, we conducted cell proliferation (Figure 4B), wound healing (Figure 4C), and tube formation assays (Figure 4D) to assess endothelial function. LY294002 significantly reversed the pro-angiogenic effects of TDAG51 knockdown. These findings confirm that the PI3K-AKT pathway mediates TDAG51-regulated angiogenesis and endothelial regeneration.

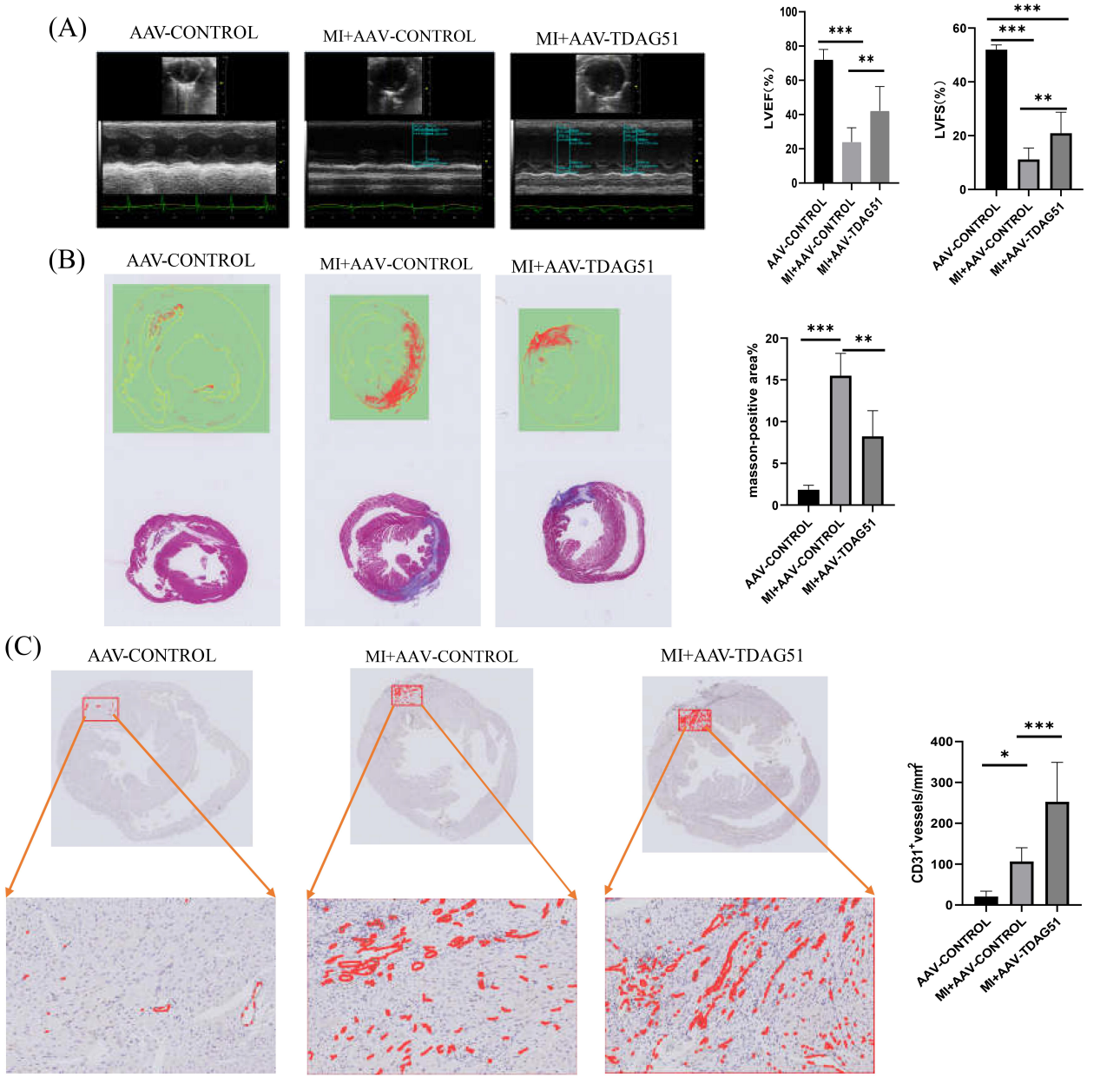


**Figure 5.** TDAG51 knock-down improved cardiac functions, decreased fibrosis and increased angiogenesis after MI. **A**) Representative images of echocardiography, and quantitative analysis of LVEF and LVFS (n≥7). **B**) Representative images and quantitative analysis of Masson staining (n≥7). **C**) Representation images and quantitative analysis of Immunohistochemical staining (n≥7). *In vivo* evidence confirms that TDAG51 inhibition protects against post-MI cardiac remodeling by promoting angiogenesis. *p<0.05, **$p$<0.01, ***$p$<0.001.

### TDAG51 knock-down ameliorates cardiac dysfunction after MI

To suppress TDAG51 expression in the mouse heart, AAV9 vectors carrying TDAG51 shRNA were directly injected into the myocardium. Two weeks later, MI was induced. Echocardiography showed that TDAG51 knockdown significantly improved cardiac function compared with MI mice (Figure 5A). Given that necrotic cardiomyocytes are replaced by fibrotic tissue, Masson's trichrome staining was used to evaluate myocardial fibrosis. The results demonstrated that TDAG51 knockdown significantly reduced fibrosis in the infarcted hearts, indicating a smaller infarct size in the TDAG51-silenced group (Figure 5B). To further elucidate the underlying mechanisms, immunohistochemical staining for CD31 was performed. Mice in the TDAG51 knockdown group exhibited increased capillary density, suggesting enhanced angiogenesis (Figure 5C). Collectively, these findings support the cardioprotective role of TDAG51 silencing in mitigating post-MI cardiac dysfunction through the promotion of angiogenesis and attenuation of fibrosis.

## Discussion

Our study demonstrates that TDAG51 expression is significantly upregulated in endothelial cells following myocardial infarction. Notably, its downregulation enhances angiogenesis *via* the PI3K-AKT signaling pathway, ultimately leading to improved cardiac function. These findings suggest that TDAG51 may serve as a promising therapeutic target for myocardial infarction.

Previous studies have reported the upregulation of TDAG51 expression in myocardial cells of myocardial infarction models.[23] In addition, the ischemia-reperfusion model of TDAG51 gene knockout mice showed improved myocardial tissue morphology, reduced infarction area, decreased myocardial cell apoptosis, and down-regulation of apoptosis-related genes.[24] The pathophysiological processes after myocardial infarction include overlapping stages of inflammation, fibrosis and angiogenesis.[5,25] Ischemia-hypoxia can trigger cardiomyocyte apoptosis within several hours to several days, accompanied by local immune cell infiltration and the release of pro-inflammatory cytokines/chemokines, thereby triggering tissue inflammation.[25,26] Subsequent bone marrow cell recruitment and proinflammatory signaling activate fibroblast collagen production and endothelial pro-angiogenic pathways.[5,25-27] The new capillaries not only deliver nutrients to the infarct boundary area, but also provide energy for the differentiation of fibroblasts into myofibroblasts - both are key to maintaining the structural and functional integrity of the heart through compensatory mechanisms.[5,25] Considering the multicellular involvement of remodeling after myocardial infarction, we hypothesize that the alterations of TDAG51 may occur not only in cardiomyocytes but also in endothelial cells. Our research results confirmed this hypothesis. Through CD31 staining and Western blot analysis, it was confirmed that the expression of TDAG51 was significantly upregulated in the myocardial infarction response, especially in the endothelial cells of the infarcted area. This upregulation indicates that TDAG51 may play a key role in the vascular response of ischemic injury and may affect endothelial function and vascular homeostasis. Similar to several well-known negative angiogenesis regulators such as PTEN and TSP-1, TDAG51 acts as a potent inhibitor of post-MI angiogenesis.[27,28] Unlike some general suppressors, TDAG51 functions specifically in endothelial cells, supporting its potential as a vascular-selective therapeutic target.

RNA sequencing data show that the knockdown of TDAG51 in HCAECs significantly alters the expression of genes related to proliferation, locomotion and growth. It is notable that we observed a significant enrichment of genes involved in the PI3K-AKT signaling pathway, indicating that TDAG51 may regulate endothelial function through this pathway. More and more evidence indicates that the activation of PI3K-AKT is involved in physiological processes such as survival, proliferation, apoptosis and migration.[29-32] The activation of the PI3K-AKT pathway creates an ideal survival environment for endothelial cells and promotes the continuous proliferation, migration and tube formation of endothelial cells,[33-35] which is consistent with the angiogenic effect observed by TDAG51 knockdown. Mechanistically, TDAG51 may act as an upstream suppressor of the PI3K-AKT signaling pathway. It could interfere with PI3K phosphorylation or recruit negative regulatory proteins to dampen pathway activation. Besides PI3K-AKT, our transcriptomic analysis implied potential involvement of MAPK/ERK and Notch signaling. These pathways will be examined in future studies.

Since proliferation, migration and angiogenesis are key processes of angiogenesis,[36] our *in vitro* experiments further demonstrated that knockdown of TDAG51 could significantly enhance these critical endothelial functions. The phosphorylation of AKT in TDAG51-knockdown cells increased, and the angiogenic effect was weakened after treatment with the PI3K inhibitor LY294002, confirming the central mediating role of the PI3K-AKT pathway. These results indicate that TDAG51 negatively regulates angiogenesis by inhibiting the PI3K-AKT signal and knocking it down becomes a potential strategy to promote angiogenesis in ischemic diseases such as myocardial infarction.

Ischemia and hypoxia after myocardial infarction change the metabolism of myocardial cells,[37] and the subsequent energy consumption causes systolic dysfunction.[38] Impaired systolic function with a low ejection fraction is associated with an increased risk of fatal arrhythmias,[39] while improved systolic function can reduce the incidence of arrhythmias and delay the progression of heart failure.[40] Myocardial fibrosis and scar tissue infiltration caused by persistent ischemia directly led to electrical conduction disorders,[41] The persistent fibrotic response results in poor remodeling and functional decline, eventually leading to heart failure,[42] all of which significantly affect the prognosis of myocardial infarction. The benefits of TDAG51 gene knockout are not limited to angiogenesis, but also include the improvement of cardiac function after myocardial infarction. Echocardiography showed that in the gene knockout group, the LVEF was enhanced, the infarction area and fibrosis were reduced, indicating better cardiac recovery. The immunohistochemical results showed an increase in the vascular density of the infarcted myocardium, further supporting the angiogenic effect of TDAG51 gene knockout, which is conducive to tissue repair and functional recovery, highlighting its therapeutic potential in improving cardiac dysfunction after myocardial infarction. In conclusion, our study identifies TDAG51 as a negative regulator of endothelial function and angiogenesis. Its upregulation after myocardial infarction may hinder vascular and cardiac recovery. Inhibiting TDAG51 promotes angiogenesis and improves cardiac function via activation of the PI3K-AKT pathway, highlighting its potential as a therapeutic target for ischemic heart disease. Future studies should further elucidate its molecular mechanisms and evaluate its translational value in preclinical and clinical settings. Targeting TDAG51 may represent a novel strategy to enhance vascular repair and improve outcomes in myocardial infarction and related cardiovascular conditions.

## References


1. Anderson JL, Morrow DA. Acute myocardial infarction. N Engl J Med 2017;376:2053-64.
2. Reed GW, Rossi JE, Cannon CP. Acute myocardial infarction. Lancet 2017;389:197-210.
3. White HD, Chew DP. Acute myocardial infarction. Lancet 2008;372:570-84.
4. Lindahl B, Mills NL. A new clinical classification of acute myocardial infarction. Nat Med 2023;29:2200-5.
5. Wu X, Reboll MR, Korf-Klingebiel M, Wollert KC. Angiogenesis after acute myocardial infarction. Cardiovasc Res 2021;117:1257-73.
6. Wang X, Zhang F, Zhang C, Zheng L, Yang J. The biomarkers for acute myocardial infarction and heart failure. Biomed Res Int 2020;2020:2018035.
7. Pfeffer MA, Claggett B, Lewis EF, Granger CB, Køber L, Maggioni AP, et al. Angiotensin receptor-neprilysin inhibition in acute myocardial infarction. N Engl J Med 2021;385:1845-55.
8. Wu X, Xiao B. TDAG51 Attenuates impaired lipid metabolism and insulin resistance in gestational diabetes mellitus through SREBP-1/ANGPTL8 pathway. Balk Med J 2023;40:175-81.
9. Platko K, Lebeau PF, Gyulay G, Lhoták Š, MacDonald ME, Pacher G, et al. TDAG51 (T-cell death-associated gene 51) is a key modulator of vascular calcification and osteogenic transdifferentiation of arterial smooth muscle cells. Arterioscler Thromb Vasc Biol 2020;40:1664-79.
10. Carlisle RE, Mohammed-Ali Z, Lu C, Yousof T, Tat V, Nademi S, et al. TDAG51 induces renal interstitial fibrosis through modulation of TGF-β receptor 1 in chronic kidney disease. Cell Death Dis 2021;12:921.
11. Hu R, Liu S, Shen W, Chen C, Cao Y, Su Z, et al. Study on the inhibitory effects of naringenin-loaded nanostructured lipid carriers against nonalcoholic fatty liver disease. J Biomed Nanotechnol 2021;17:942-51.
12. Wu J, Zhang W, Li C. Recent advances in genetic and epigenetic modulation of animal exposure to high temperature. Front Genet 2020;11:653.
13. Xu J, Jiang J, Li X, Yu X, Xu Y, Lu Y. Comparative transcriptomic analysis of vascular endothelial cells after hypoxia/reoxygenation induction based on microarray technology. J Zhejiang Univ Sci B 2020;21:291-304.
14. Carlisle RE, Mohammed-Ali Z, Lu C, Yousof T, Tat V, Nademi S, et al. TDAG51 induces renal interstitial fibrosis through modulation of TGF-β receptor 1 in chronic kidney disease. Cell Death Dis 2021;12:921.
15. Platko K, Gyulay G, Lebeau PF, MacDonald ME, Lynn EG, Byun JH, et al. GDF10 is a negative regulator of vascular calcification. J Biol Chem 2024;300:107805.
16. Sanchez-Margálet V, Goldfine ID, Vlahos CJ, Sung CK. Role of phosphatidylinositol-3-kinase in insulin receptor signaling: studies with inhibitor, LY294002. Biochem Bioph Res Commun 1994;204:446-52.
17. Yue Y, Yang X, Feng K, Wang L, Hou J, Mei B, et al. Corrigendum to "M2b macrophages reduce early reperfusion injury after myocardial ischemia in mice: A predominant role of inhibiting apoptosis via A20" [Int. J. Cardiol. 245 (2017) 228-235]. Int J Cardiol 2019;278:311.
18. Yue Y, Yang X, Feng K, Wang L, Hou J, Mei B, et al. M2b macrophages reduce early reperfusion injury after myocardial ischemia in mice: A predominant role of inhibiting apoptosis via A20. Int J Cardiol 2017;245:228-35.
19. Yue Y, Huang S, Wang L, Wu Z, Liang M, Li H, et al. M2b macrophages regulate cardiac fibroblast activation and alleviate cardiac fibrosis after reperfusion injury. Circ J 2020;84:626-35.
20. Yue Y, Huang S, Li H, Li W, Hou J, Luo L, et al. M2b macrophages protect against myocardial remodeling after ischemia/reperfusion injury by regulating kinase activation of platelet-derived growth factor receptor of cardiac fibroblast. Ann Transl Med 2020;8:1409.
21. Wang C, Yue Y, Huang S, Wang K, Yang X, Chen J, et al. M2b macrophages stimulate lymphangiogenesis to reduce myocardial fibrosis after myocardial ischaemia/reperfusion injury. Pharm Biol 2022;60:384-93.
22. Chen C, Wang J, Liu C, Hu J, Liu L. Pioneering therapies for post-infarction angiogenesis: Insight into molecular mechanisms and preclinical studies. Biomed Pharmacother 2023;166:115306.
23. Wang J, Wang F, Zhu J, Song M, An J, Li W. Transcriptome profiling reveals PHLDA1 as a novel molecular marker for ischemic cardiomyopathy. J Mol Neurosci 2018;65:102-9.
24. Guo Y, Jia P, Chen Y, Yu H, Xin X, Bao Y, et al. PHLDA1 is a new therapeutic target of oxidative stress and ischemia reperfusion-induced myocardial injury. Life Sci 2020;245:117347.
25. Fraccarollo D, Galuppo P, Bauersachs J. Novel therapeutic approaches to post-infarction remodelling. Cardiovasc Res 2012;94:293-303.
26. Viola M, de Jager SCA, Sluijter JPG. Targeting inflammation after myocardial infarction: a therapeutic opportunity for extracellular vesicles? Int J Mol Sci 2021;22:7831.
27. Jeo WS, Lalisang TJM, Siregar NC, et al. Semiquantitative assessment of phosphatase and tensin homolog value with immunohistochemistry in colorectal cancer. Int J Biol Markers 2024;39:248-54.
28. Jung M, Dodsworth M, Thum T. Inflammatory cells and their non-coding RNAs as targets for treating myocardial infarction. Basic Res Cardiol 2018;114:4.
29. Ronnebaum SM, Patterson C. The FoxO family in cardiac function and dysfunction. Annu Rev Physiol 2010;72:81-94.
30. Razavi HM, Hamilton JA, Feng Q. Modulation of apoptosis by nitric oxide: implications in myocardial ischemia and heart failure. Pharmacol Therapeut 2005;106:147-62.
31. Sciarretta S, Forte M, Frati G, Sadoshima J. New insights into the role of mTOR signaling in the cardiovascular system. Circ Res 2018;122:489-505.
32. Ghigo A, Laffargue M, Li M, Hirsch E. PI3K and calcium signaling in cardiovascular disease. Circ Res 2017;121:282-92.
33. Dvorak HF. Angiogenesis: update 2005. J Thromb Haemost 2005;3:1835-42.
34. Davies EM, Gurung R, Le KQ, Mitchell CA. Effective angiogenesis requires regulation of phosphoinositide signaling. Adv Biol Regul 2019;71:69-78.
35. Potente M, Carmeliet P. The link between angiogenesis and endothelial metabolism. Annu Rev Physiol 2017;79:43-66.
36. Pugh CW. Modulation of the hypoxic response. Adv Exp Med Biol 2016;903:259-71.
37. Rosano GMC, Fini M, Caminiti G, Barbaro G. Cardiac metabolism in myocardial ischemia. Curr Pharm Design 2008;14:2551-62.
38. Janse MJ, Wit AL. Electrophysiological mechanisms of ventricular arrhythmias resulting from myocardial ischemia and infarction. Physiol Rev 1989;69:1049-169.
39. Hallstrom A, Pratt CM, Greene HL, Huther M, Gottlieb S,

DeMaria A, et al. Relations between heart failure, ejection fraction, arrhythmia suppression and mortality: analysis of the Cardiac Arrhythmia Suppression Trial. J Am Coll Cardiol 1995;25:1250-7.
40. Marks AR. Calcium cycling proteins and heart failure: mechanisms and therapeutics. J Clin Invest 2013;123:46-52.
41. Frangogiannis NG. Cardiac fibrosis. Cardiovasc Res 2021;117:1450-88.
42. Piek A, de Boer RA, Silljé HHW. The fibrosis-cell death axis in heart failure. Heart Fail Rev 2016;21:199-211.

Received: 29 March 2026. Accepted: 20 May 2026.


*European Journal of Histochemistry 2026; 70:4569*
*doi:10.4081/ejh.2026.4569*